

Search for evidence of neutron fluxes using Pierre Auger Observatory data

Danelise de Oliveira Franco^{a,*} for the Pierre Auger Collaboration^b

^aState University of Campinas, Gleb Wataghin Institute of Physics,
Rua Sérgio Buarque de Holanda, 777, Campinas, Brazil

^bObservatorio Pierre Auger,
Av. San Martín Norte 304, 5613 Malargüe, Argentina

Full author list: https://www.auger.org/archive/authors_icrc_2023.html

E-mail: spokespersons@auger.org

Astrophysical neutral particles, such as neutrons, can point directly to their sources since they are not affected by magnetic fields. We expect neutron production in the immediate vicinity of the acceleration sites due to cosmic ray interactions. Hence, a high-energy neutron flux could help to identify sources of cosmic rays in the EeV range. Free neutrons, although unstable, can travel a mean distance of 9.2 kpc times their energy in EeV. Due to the neutron instability, we limit the searches to Galactic candidate sources. Since air showers initiated by a neutron are indistinguishable from those generated by a proton, we would recognize a neutron flux as an excess of events from the direction of its source. Previous searches using events with a zenith angle up to 60° and energies above 1 EeV found no surplus of events that would indicate a neutron flux. We present the results of the search for evidence of high-energy neutron fluxes using a data set about three times larger than the previous work. We investigate the sky in the field of view of the Pierre Auger Observatory, narrowing down to specific directions of candidate sources. With respect to previous works, we extend the angular range up to zenith angles of 80°, reaching declinations from -90° to +45°, and the energy range going as low as 0.1 EeV. The extension in the field of view provides exposure to the Crab Nebula for the first time.

38th International Cosmic Ray Conference (ICRC2023)
26 July - 3 August, 2023
Nagoya, Japan



*Speaker

1. Introduction

One central open question regarding ultra-high-energy cosmic rays is the identification of their sources. Since charged particles are deflected by interstellar magnetic fields, the identification of the sources based only on their arrival directions can be challenging, although some breakthroughs have been obtained in the past decade [1]. On the other hand, the arrival directions of neutral particles point directly to their sources, making neutral particles a powerful tool in the investigation of cosmic ray sources. Even though free neutrons undergo β -decay with a mean lifetime of around 879 s [2], they travel a distance around $9.2 \text{ kpc}(E/\text{EeV})$ in the ultra-relativistic regime. Therefore, considering the possible traveled distance, we can investigate neutron fluxes in the EeV range from Galactic sources.

The production of ultra-high-energy protons from a source is expected to be accompanied by the generation of neutrons. These neutrons can be generated through pion production processes or nuclear photodisintegrations near the source. A possible mechanism to produce neutrons is ultra-high-energy proton collisions with ambient protons or photons [3]. Since neutron production mechanisms can lead to associated γ -ray production, we can explore γ -ray sources as potential candidates for EeV neutron sources.

In previous publications in which the Pierre Auger Collaboration searched for neutron fluxes [4, 5], no statistically significant results were obtained. In this work, we include nine more years of observation with respect to [5]. Additionally, we also include events with a zenith angle between 60° and 80° , expanding the field of view from a maximum declination of $+25^\circ$ to $+45^\circ$. The total exposure increased from $36,000 \text{ km}^2 \text{ sr yr}$ to $110,000 \text{ km}^2 \text{ sr yr}$, considering the array in which the detectors are spaced 1,500 m from each other. In this analysis, we also consider events with energies down to 0.1 EeV, recorded using the surface detector sub-array with a 750 m spacing, with a total exposure of $408 \text{ km}^2 \text{ sr yr}$.

2. Data sets

The Pierre Auger Observatory [6] is located in Argentina, near the city of Malargüe. The water-Cherenkov stations form an array, called the Surface Detector (SD), covering an area of about $3,000 \text{ km}^2$ arranged in a triangular grid with 1,500 m spacing. We use events recorded with the SD from 2004 January 1 to 2022 December 31. We consider those recorded by the 1,500 m SD array with zenith angles up to 80° , resulting in declination values between -90° and $+45^\circ$. This data set contains more than 2,650,000 events, and we split them into the same four energy ranges used in the previous neutron searches: $1 \text{ EeV} \leq E < 2 \text{ EeV}$, $2 \text{ EeV} \leq E < 3 \text{ EeV}$, $E \geq 3 \text{ EeV}$, and the cumulative data set $E \geq 1 \text{ EeV}$. We also use a data set recorded with the portion of the array in which the detectors are placed 750 m from each one, covering an area of approximately 24 km^2 [7]. These events were recorded from 2008 August 1 to 2022 December 21. The events in this data set, referred to as the “750 m data set”, extends down to a lower energy, starting at 0.1 EeV. The 750 m data set contains more than 1,500,000 events, split into the following energy ranges: $0.1 \text{ EeV} \leq E < 0.2 \text{ EeV}$, $0.2 \text{ EeV} \leq E < 0.3 \text{ EeV}$, $E \geq 0.3 \text{ EeV}$, and the cumulative data set $E \geq 0.1 \text{ EeV}$. Events recorded with the 750 m array have a zenith angle less than 55° , resulting in a declination less than

20°. For all the data sets used in this analysis, we use the most stringent selection criteria, keeping only events in which all six neighboring stations of the one with the highest signal are active.

3. Target sets

The catalogs previously used in [5] were updated. The total number of point sources considered in our analysis increased from 358 to 888. Since we expand the field of view of the analysis to declinations up to 45°, we are able to include for instance the Crab Nebula, which is potentially interesting. The catalogs used in this work include the millisecond pulsars [8], γ -ray pulsars [9], low-mass X-ray binaries [10], high-mass X-ray binaries [11], TeV γ -ray Pulsar Wind Nebulae, other identified TeV γ -ray sources, unidentified TeV γ -ray sources¹, microquasars², magnetars³ [12], and sources detected by the LHAASO Observatory as PeVatrons [13]. Two other single-element target sets are considered: the Galactic center and the Crab. The 750 m data set has events in a lower energy range between 0.1 EeV and 1 EeV. In this energy range, neutrons are expected to travel shorter lengths. Moreover, the accessible field of view using the 750 m data set is more limited when compared to the 1,500 m one. Therefore, we perform the analysis of the former data set with a reduced number of candidate sources. We keep candidate sources within a distance of 1 kpc and with a declination of less than 20°.

4. Method and results

Since an air shower initiated by a proton and one initiated by a neutron are indistinguishable, we can only identify a neutron flux through event excesses around the direction of the candidate source. While charged particles are deflected during their propagation, neutrons travel in straight lines producing a surplus pointing to their sources. We compare the observed cosmic ray density at the position of the target with the density obtained using isotropic data sets. We estimate the cosmic ray density from the probability density of each event in the data set coming from the direction of the target. We define a weight that represents the probability density of the i -th event to be associated with the j -th target as

$$w_{ij} = \frac{1}{2\pi\sigma_i^2} \exp\left(-\frac{\xi_{ij}^2}{2\sigma_i^2}\right). \quad (1)$$

This weight is based on a two-dimensional Gaussian distribution taking into account the angular distance between the i -th event and the j -th target ξ_{ij} . The parameter σ_i is estimated from the angular uncertainties measured at the Observatory. We parameterize σ in multiplicity (number of triggered stations in the air shower event) and zenith angle to avoid statistical fluctuations caused by individual events. Figure 1 shows the result of this parameterization for both data sets.

By summing the weights of all the N events in the data set, we estimate the cosmic ray density at the position of the target:

¹The PWNe, the other sources, and the unidentified sources were selected from <http://tevcat2.uchicago.edu/>.

²<http://www.aim.univ-paris7.fr/CHATY>

³<http://www.physics.mcgill.ca/~pulsar/magnetar/main.html>

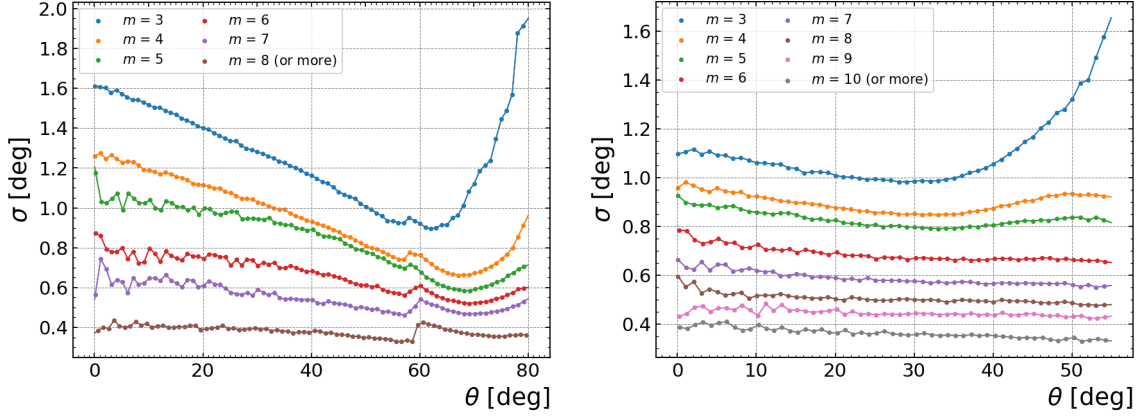


Figure 1: Parameterization of σ as a function of the zenith angle. On the left (right), we show the result obtained with the data set recorded by the 1,500 m (750 m) array. The continuous lines are the result of a linear interpolation. The multiplicity (number of triggered stations in the air shower event) is represented by m .

$$\rho_j^{\text{obs}} = \sum_i^N w_{ij}. \quad (2)$$

Then, we can compare the observed density ρ_j^{obs} with the value obtained with data sets in which local anisotropies are smoothed. We use a scrambling method to erase small-scale anisotropies while preserving the large-scale structure. To simulate an arrival direction, we randomly sample two events from the observed data set, extracting from one of those the arrival time information and from the other the zenith angle and its associated σ parameter. We also sample an azimuth angle from a uniform distribution between 0 and 2π . By taking the zenith angle and the σ parameter from the same event, we ensure we are sampling a σ distribution similar to the real one. Each simulated data set has the same number of events as the observed one. For each target, we estimate the density obtained with a scrambled data set ρ_j^{scr} . The p -value is then defined as the fraction of simulated data sets resulting in a ρ_j^{scr} larger than ρ_j^{obs} . We generate 10,000 simulated data sets to estimate the p -value. The penalized p -value, $p^* = 1 - (1 - p)^M$, takes into account the fact that in each target set, we are testing M targets. It represents the probability of getting a p -value equal to or less than p if all the M p -values were sampled from a uniform distribution between 0 and 1.

We determine an upper limit on the flux of neutrons from each target direction. First, we find the upper limit on the number of excess events from that direction. The upper limit on the flux is the upper limit on the number of recorded neutrons divided by the directional exposure. The directional exposure is obtained by dividing the expected cosmic ray density ρ_j^{exp} , defined as the mean of the ρ_j^{scr} obtained with the 10,000 simulated data sets, by the cosmic ray intensity. We estimate the cosmic ray intensity by integrating the energy spectrum [14] in the energy range of interest. We use simulated events to estimate the upper limit on the number of neutrons. A simulated event is generated by randomly sampling a σ value from the observed distribution and using it to sample an angular distance from a two-dimensional Gaussian distribution. Using the simulated angular distance and the sampled σ , we estimate the associated weight (Equation 1). We use the 10,000

simulated data sets as background and add simulated events in each data set with a step of one. Then, the upper limit on the number of neutrons is the smallest value of n added events that satisfy the condition $f_n < (1 - \text{CL})f_0$, where f_0 is the fraction of data sets in which the cosmic ray density at the position of the target is less than the observed one, f_n is this fraction after adding n events, and CL is the confidence level. For this analysis, we use a confidence level of 95%. We also estimate the energy flux upper limit, assuming an E^{-2} spectrum. In Tables 1 and 2, we present the results for the cumulative data sets obtained with events recorded by the 1,500 m and the 750 m arrays, respectively. For each class, we report the most significant target, i.e., the one with the smallest individual p -value, showing its position, the upper limit on the flux and on the energy flux, the p -value⁴ and the penalized p -value.

Table 1: Results for the most significant target in each target set using events recorded by the 1,500 m array with energies $E \geq 1$ EeV.

Class	R.A. [deg]	Dec. [deg]	Flux U.L. [km ⁻² yr ⁻¹]	E-Flux U.L. [eV cm ⁻² s ⁻¹]	p -value	p^*
msec PSRs	286.2	2.1	0.026	0.19	0.0075	0.88
γ -ray PSRs	296.6	-54.1	0.023	0.17	5.0×10^{-5}	0.013
LMXB	237.0	-62.6	0.017	0.12	0.0069	0.51
HMXB	308.1	41.0	0.13	0.97	0.014	0.57
TeV γ -ray - PWN	128.8	-45.6	0.016	0.12	0.0070	0.18
TeV γ -ray - other	128.8	-45.2	0.014	0.11	0.022	0.63
TeV γ -ray - UNID	305.0	40.8	0.15	1.1	0.0066	0.31
Microquasars	308.1	41.0	0.13	0.95	0.014	0.19
Magnetars	249.0	-47.6	0.011	0.079	0.15	0.99
LHAASO	292.3	17.8	0.038	0.28	0.024	0.20
Crab	83.6	22.0	0.020	0.15	0.71	0.71
Galactic Center	266.4	-29.0	0.0053	0.039	0.86	0.86

Table 2: Results for the most significant target in each target set using events recorded by the 750 m array with energies $E \geq 0.1$ EeV.

Class	R.A. [deg]	Dec. [deg]	Flux U.L. [km ⁻² yr ⁻¹]	E-Flux U.L. [eV cm ⁻² s ⁻¹]	p -value	p^*
msec PSRs	140.5	-52.0	1.7	12.5	0.043	0.66
γ -ray PSRs	288.4	10.3	5.3	38.9	0.0056	0.47
HMXB	116.9	-53.3	2.1	15.1	0.0092	0.071
TeV γ -ray - PWN	277.9	-9.9	1.8	13.4	0.12	0.48
TeV γ -ray - other	288.2	10.2	5.5	40.2	0.0033	0.036
Magnetars	274.7	-16.0	1.6	11.8	0.13	0.44

⁴For the specific case of the γ -ray pulsar located at (296.6°, -54.1°), we simulated 200,000 data sets to estimate the p -value.

Table 3: Results for the combined analysis for events recorded by the 1,500 m array.

Class	No.	Unweighted combined p -value P			
		≥ 1 EeV	1 – 2 EeV	2 – 3 EeV	≥ 3 EeV
msec PSRs	283	0.90	0.79	0.20	1.0
γ -ray PSRs	261	0.16	0.12	0.50	0.86
LMXB	102	0.62	0.89	0.11	0.55
HMXB	60	0.49	0.46	0.28	0.85
TeV γ -ray - PWN	28	0.24	0.52	0.072	0.49
TeV γ -ray - other	45	0.52	0.81	0.15	0.34
TeV γ -ray - UNID	56	0.61	0.85	0.57	0.40
Microquasars	15	0.39	0.49	0.50	0.68
Magnetars	27	0.99	0.99	0.85	0.67
LHAASO	9	0.22	0.31	0.54	0.31
Crab	1	0.71	0.54	0.30	0.93
Galactic Center	1	0.86	0.78	0.72	0.67

Table 4: Results for the combined analysis including statistical weights for events recorded by the 1,500 m array.

Class	No.	Weighted combined p -value P_ω			
		≥ 1 EeV	1 – 2 EeV	2 – 3 EeV	≥ 3 EeV
msec PSRs	283	0.50	0.82	0.0093	0.81
γ -ray PSRs	261	0.020	0.0068	0.31	0.61
LMXB	102	0.25	0.79	0.44	0.067
HMXB	60	0.34	0.25	0.66	0.42
TeV γ -ray - PWN	28	0.0052	0.0072	0.035	0.51
TeV γ -ray - other	45	0.22	0.55	0.30	0.15
TeV γ -ray - UNID	56	0.75	0.94	0.67	0.23
Microquasars	15	0.81	0.85	0.75	0.38
Magnetars	27	0.98	0.95	0.78	0.90
LHAASO	9	0.42	0.60	0.43	0.35

We also tested each class of candidate sources as a target. If one class of these target sets is emitting neutrons, it would be more significant when combining all the individual sources than when looking at the individual objects. The chance probability of a product of M p -values sampled from a uniform distribution (Π) not to be greater than the actual product of the M individual p -values (Π_0) is given by

$$\mathcal{P}(\Pi \leq \Pi_0) = \Pi_0 \sum_{k=0}^{M-1} \frac{(-\ln \Pi_0)^k}{k!} = 1 - \text{Poisson}(M, -\ln \Pi_0), \quad (3)$$

where $\text{Poisson}(M, -\ln \Pi_0)$ represents the probability of getting M or more targets in the presence of a background following a Poisson distribution with mean $-\ln \Pi_0$. We also can include statistical

Table 5: Results for the combined analysis for events recorded by the 750 m array.

Class	No.	Unweighted combined p -value P			
		≥ 0.1 EeV	$0.1 - 0.2$ EeV	$0.2 - 0.3$ EeV	≥ 0.3 EeV
msec PSRs	25	0.82	0.41	0.90	0.67
γ -ray PSRs	113	0.53	0.70	0.29	0.38
HMXB	8	0.33	0.68	0.069	0.28
TeV γ -ray - PWN	5	0.43	0.72	0.12	0.36
TeV γ -ray - other	11	0.074	0.55	0.070	0.16
Magnetars	4	0.31	0.48	0.26	0.21

Table 6: Results for the combined analysis including statistical weights for events recorded by the 750 m array.

Class	No.	Weighted combined p -value P_ω			
		≥ 0.1 EeV	$0.1 - 0.2$ EeV	$0.2 - 0.3$ EeV	≥ 0.3 EeV
msec PSRs	25	0.58	0.48	0.95	0.15
γ -ray PSRs	113	0.93	0.94	0.85	0.14
HMXB	8	0.23	0.79	0.22	0.029
TeV γ -ray - PWN	5	0.83	0.96	0.73	0.11
TeV γ -ray - other	11	0.58	0.82	0.22	0.44
Magnetars	4	0.14	0.35	0.046	0.40

weights for each one of the targets. Each statistical weight is proportional to the exposure of the Observatory in that location, to the electromagnetic flux of the target, and to its expected flux attenuation factor due to neutron decay, considering the traveled distance⁵. After evaluating the statistical weight for each target, we normalize the weights so that their sum is equal to 1 in each target set. The weighted product Π_0^ω is the product obtained using all the individual p -values raised to the power of its corresponding statistical weight. We used simulated sets of M individual p -values sampled from a uniform distribution between 0 and 1 and raised to their corresponding statistical weight to obtain the product Π^ω . The weighted combined p -value is the fraction of simulated Π^ω that are less than Π_0^ω . Tables 3 and 4 (5 and 6) show the results for the combined analysis without and including the statistical weights for events recorded by the 1,500 m (750 m) array for all energy ranges.

5. Conclusions

We did not find clear evidence for a neutron flux coming from any of the tested candidate sources in any of the energy ranges, strengthening results previously published by the Auger Collaboration. The results do not exclude the existence of EeV neutrons from some of these Galactic sources with flux levels at Earth that are below our upper limits. Moreover, our time-averaged upper limits

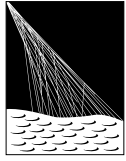
⁵If we do not have information about the distance, the statistical weight is evaluated based on the other two pieces of information.

pertain to steady sources and do not constrain short outbursts. In the future, we plan to search for correlations with transient emissions of high-energy photons from Galactic sources recorded by other observatories. We also plan to perform an updated blind search for a neutron flux from any direction of the sky in a forthcoming work.

References

- [1] G. Golup [Pierre Auger coll.], PoS(ICRC2023)252.
- [2] R. L. Workman et al. [Particle Data Group], *Prog. Theor. Exp. Phys* **2022** (2022) and 2023 update 083C01.
- [3] G. A. Medina-Tanco and A. A. Watson, Proc. 27th ICRC (2001), 531.
- [4] The Pierre Auger Collaboration, *ApJ* **760** (2012) 148 [1211.4901].
- [5] The Pierre Auger Collaboration, *ApJL* **789** (2014) L34 [1406.4038].
- [6] The Pierre Auger Collaboration, *Nucl. Instrum. Meth. A* **798** (2015) 172 [1502.01323].
- [7] The Pierre Auger Collaboration, *JINST* **16** (2021) T07008 [2101.11747].
- [8] R. N. Manchester et al., *AJ* **129** (2005) 1993.
- [9] A. A. Abdo et al., *ApJS* **208** (2013) 17 [1305.4385].
- [10] Q. Z. Liu et al., *A&A* **469** (2007) 807 [0707.0544].
- [11] Q. Z. Liu et al., *A&A* **455** (2006) 1165 [0707.0549].
- [12] S. A. Olausen and V. M. Kaspi, *ApJS* **212** (2014) 6 [1309.4167].
- [13] Z. Cao et al., *Nature* **594** (2021) 33.
- [14] The Pierre Auger Collaboration, *Phys. Rev. D* **102** (2020) 062005 [2008.06486].

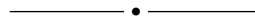
The Pierre Auger Collaboration



PIERRE
AUGER
OBSERVATORY

A. Abdul Halim¹³, P. Abreu⁷², M. Aglietta^{54,52}, I. Allekotte¹, K. Almeida Cheminant⁷⁰, A. Almela^{7,12}, R. Aloisio^{45,46}, J. Alvarez-Muñiz⁷⁹, J. Ammerman Yebra⁷⁹, G.A. Anastasi^{54,52}, L. Anchordoqui⁸⁶, B. Andrada⁷, S. Andringa⁷², C. Aramo⁵⁰, P.R. Araújo Ferreira⁴², E. Arnone^{63,52}, J. C. Arteaga Velázquez⁶⁷, H. Asorey⁷, P. Assis⁷², G. Avila¹¹, E. Avocone^{57,46}, A.M. Badescu⁷⁵, A. Bakalova³², A. Balaceanu⁷³, F. Barbato^{45,46}, A. Bartz Mocellin⁸⁵, J.A. Bellido^{13,69}, C. Berat³⁶, M.E. Bertaina^{63,52}, G. Bhatta⁷⁰, M. Bianciotto^{63,52}, P.L. Biermann^h, V. Binet⁵, K. Bismark^{39,7}, T. Bister^{80,81}, J. Biteau³⁷, J. Blazek³², C. Bleve³⁶, J. Blümer⁴¹, M. Boháčová³², D. Boncioli^{57,46}, C. Bonifazi^{8,26}, L. Bonneau Arbeletche²¹, N. Borodai⁷⁰, J. Brack^j, P.G. Bricchetto Orcherá⁷, F.L. Briechele⁴², A. Bueno⁷⁸, S. Buitink¹⁵, M. Buscemi^{47,61}, M. Büsken^{39,7}, A. Bwembya^{80,81}, K.S. Caballero-Mora⁶⁶, S. Cabana-Freire⁷⁹, L. Caccianiga^{59,49}, I. Caracas³⁸, R. Caruso^{58,47}, A. Castellina^{54,52}, F. Catalani¹⁸, G. Cataldi⁴⁸, L. Cazon⁷⁹, M. Cerda¹⁰, A. Cermenati^{45,46}, J.A. Chinellato²¹, J. Chudoba³², L. Chytka³³, R.W. Clay¹³, A.C. Cobos Cerutti⁶, R. Colalillo^{60,50}, A. Coleman⁹⁰, M.R. Coluccia⁴⁸, R. Conceição⁷², A. Condorelli³⁷, G. Consolati^{49,55}, M. Conte^{56,48}, F. Convenga⁴¹, D. Correia dos Santos²⁸, P.J. Costa⁷², C.E. Covault⁸⁴, M. Cristinziani⁴⁴, C.S. Cruz Sanchez³, S. Dasso^{4,2}, K. Daumiller⁴¹, B.R. Dawson¹³, R.M. de Almeida²⁸, J. de Jesús^{7,41}, S.J. de Jong^{80,81}, J.R.T. de Mello Neto^{26,27}, I. De Mitri^{45,46}, J. de Oliveira¹⁷, D. de Oliveira Franco²¹, F. de Palma^{56,48}, V. de Souza¹⁹, E. De Vito^{56,48}, A. Del Popolo^{58,47}, O. Deligny³⁴, N. Denner³², L. Deval^{41,7}, A. di Matteo⁵², M. Dobre⁷³, C. Dobrigkeit²¹, J.C. D'Olivo⁶⁸, L.M. Domingues Mendes⁷², J.C. dos Anjos, R.C. dos Anjos²⁵, J. Ebr³², F. Ellwanger⁴¹, M. Emam^{80,81}, R. Engel^{39,41}, I. Epicoco^{56,48}, M. Erdmann⁴², A. Etchegoyen^{7,12}, C. Evoli^{45,46}, H. Falcke^{80,82,81}, J. Farmer⁸⁹, G. Farrar⁸⁸, A.C. Fauth²¹, N. Fazzini^e, F. Feldbusch⁴⁰, F. Fenu^{41,d}, A. Fernandes⁷², B. Fick⁸⁷, J.M. Figueira⁷, A. Filipčič^{77,76}, T. Fitoussi⁴¹, B. Flaggs⁹⁰, T. Fodran⁸⁰, T. Fujii^{89,f}, A. Fuster^{7,12}, C. Galea⁸⁰, C. Galelli^{59,49}, B. García⁶, C. Gaudu³⁸, H. Gemmeke⁴⁰, F. Gesualdi^{7,41}, A. Gherghel-Lascu⁷³, P.L. Ghia³⁴, U. Giaccari⁴⁸, M. Giammarchi⁴⁹, J. Glombitza^{42,g}, F. Gobbi¹⁰, F. Gollan⁷, G. Golup¹, M. Gómez Berisso¹, P.F. Gómez Vitale¹¹, J.P. Gongora¹¹, J.M. González¹, N. González⁷, I. Goos¹, D. Góra⁷⁰, A. Gorgi^{54,52}, M. Gottowik⁷⁹, T.D. Grubb¹³, F. Guarino^{60,50}, G.P. Guedes²², E. Guido⁴⁴, S. Hahn³⁹, P. Hamal³², M.R. Hampel⁷, P. Hansen³, D. Harari¹, V.M. Harvey¹³, A. Haungs⁴¹, T. Hebbeker⁴², C. Hojvat^e, J.R. Hörandel^{80,81}, P. Horvath³³, M. Hrabovský³³, T. Huege^{41,15}, A. Insolia^{58,47}, P.G. Isar⁷⁴, P. Janecek³², J.A. Johnsen⁸⁵, J. Jurysek³², A. Kääpä³⁸, K.H. Kampert³⁸, B. Keilhauer⁴¹, A. Khakurdikar⁸⁰, V.V. Kizakke Covilakam^{7,41}, H.O. Klages⁴¹, M. Kleifges⁴⁰, F. Knapp³⁹, N. Kunka⁴⁰, B.L. Lago¹⁶, N. Langner⁴², M.A. Leigui de Oliveira²⁴, Y. Lema-Capeans⁷⁹, V. Lenok³⁹, A. Letessier-Selvon³⁵, I. Lhenry-Yvon³⁴, D. Lo Presti^{58,47}, L. Lopes⁷², L. Lu⁹¹, Q. Luce³⁹, J.P. Lundquist⁷⁶, A. Machado Payeras²¹, M. Majercakova³², D. Mandat³², B.C. Manning¹³, P. Mantsch^e, S. Marafico³⁴, F.M. Mariani^{59,49}, A.G. Mariazzi³, I.C. Mariş¹⁴, G. Marsella^{61,47}, D. Martello^{56,48}, S. Martinelli^{41,7}, O. Martínez Bravo⁶⁴, M.A. Martins⁷⁹, M. Mastrodicasa^{57,46}, H.J. Mathes⁴¹, J. Matthews^a, G. Matthiae^{62,51}, E. Mayotte^{85,38}, S. Mayotte⁸⁵, P.O. Mazur^e, G. Medina-Tanco⁶⁸, J. Meinert³⁸, D. Melo⁷, A. Menshikov⁴⁰, C. Merx⁴¹, S. Michal³³, M.I. Micheletti⁵, L. Miramonti^{59,49}, S. Mollerach¹, F. Montanet³⁶, L. Morejon³⁸, C. Morello^{54,52}, A.L. Müller³², K. Mulrey^{80,81}, R. Mussa⁵², M. Muzio⁸⁸, W.M. Namasaka³⁸, S. Negi³², L. Nellen⁶⁸, K. Nguyen⁸⁷, G. Nicora⁹, M. Niculescu-Oglinزانu⁷³, M. Niechciol⁴⁴, D. Nitz⁸⁷, D. Nosek³¹, V. Novotny³¹, L. Nožka³³, A. Nucita^{56,48}, L.A. Núñez³⁰, C. Oliveira¹⁹, M. Palatka³², J. Pallotta⁹, S. Panja³², G. Parente⁷⁹, T. Paulsen³⁸, J. Pawlowsky³⁸, M. Pech³², J. Pečala⁷⁰, R. Pelayo⁶⁵, L.A.S. Pereira²³, E.E. Pereira Martins^{39,7}, J. Perez Armand²⁰, C. Pérez Bertolli^{7,41}, L. Perrone^{56,48}, S. Petrera^{45,46}, C. Petrucci^{57,46}, T. Pierog⁴¹, M. Pimenta⁷², M. Platino⁷, B. Pont⁸⁰, M. Pothast^{81,80}, M. Pourmohammad Shahvar^{61,47}, P. Privitera⁸⁹, M. Prouza³², A. Puyleart⁸⁷, S. Querchfeld³⁸, J. Rautenberg³⁸, D. Ravnani⁷, M. Reininghaus³⁹, J. Ridky³², F. Riehn⁷⁹, M. Risse⁴⁴, V. Rizi^{57,46}, W. Rodrigues de Carvalho⁸⁰, E. Rodriguez^{7,41}, J. Rodriguez Rojo¹¹, M.J. Roncoroni⁷, S. Rossoni⁴³, M. Roth⁴¹, E. Roulet¹, A.C. Rovero⁴, P. Ruehl⁴⁴, A. Saftoiu⁷³, M. Saharan⁸⁰, F. Salamida^{57,46}, H. Salazar⁶⁴, G. Salina⁵¹, J.D. Sanabria Gomez³⁰, F. Sánchez⁷, E.M. Santos²⁰, E. Santos³²,

F. Sarazin⁸⁵, R. Sarmiento⁷², R. Sato¹¹, P. Savina⁹¹, C.M. Schäfer⁴¹, V. Scherini^{56,48}, H. Schieler⁴¹, M. Schimassek³⁴, M. Schimp³⁸, F. Schlüter⁴¹, D. Schmidt³⁹, O. Scholten^{15,i}, H. Schoorlemmer^{80,81}, P. Schovánek³², F.G. Schröder^{90,41}, J. Schulte⁴², T. Schulz⁴¹, S.J. Sciutto³, M. Scornavacche^{7,41}, A. Segreto^{53,47}, S. Sehgal³⁸, S.U. Shivashankara⁷⁶, G. Sigl⁴³, G. Silli⁷, O. Sima^{73,b}, F. Simon⁴⁰, R. Smau⁷³, R. Šmída⁸⁹, P. Sommers^k, J.F. Soriano⁸⁶, R. Squartini¹⁰, M. Stadelmaier³², D. Stanca⁷³, S. Stanič⁷⁶, J. Stasielak⁷⁰, P. Stassi³⁶, S. Strähnz³⁹, M. Straub⁴², M. Suárez-Durán¹⁴, T. Suomijärvi³⁷, A.D. Supanitsky⁷, Z. Svozilikova³², Z. Szadkowski⁷¹, A. Tapia²⁹, C. Taricco^{63,52}, C. Timmermans^{81,80}, O. Tkachenko⁴¹, P. Tobiska³², C.J. Todero Peixoto¹⁸, B. Tomé⁷², Z. Torrès³⁶, A. Travaini¹⁰, P. Travnicek³², C. Trimarelli^{57,46}, M. Tueros³, M. Unger⁴¹, L. Vaclavěk³³, M. Vacula³³, J.F. Valdés Galicia⁶⁸, L. Valore^{60,50}, E. Varela⁶⁴, A. Vásquez-Ramírez³⁰, D. Veberič⁴¹, C. Ventura²⁷, I.D. Vergara Quispe³, V. Verzi⁵¹, J. Vicha³², J. Vink⁸³, J. Vlastimil³², S. Vorobiov⁷⁶, C. Watanabe²⁶, A.A. Watson^c, A. Weindl⁴¹, L. Wiencke⁸⁵, H. Wilczyński⁷⁰, D. Wittkowski³⁸, B. Wundheiler⁷, B. Yue³⁸, A. Yushkov³², O. Zapparrata¹⁴, E. Zas⁷⁹, D. Zavrtanik^{76,77}, M. Zavrtanik^{77,76}



- ¹ Centro Atómico Bariloche and Instituto Balseiro (CNEA-UNCuyo-CONICET), San Carlos de Bariloche, Argentina
- ² Departamento de Física and Departamento de Ciencias de la Atmósfera y los Océanos, FCEyN, Universidad de Buenos Aires and CONICET, Buenos Aires, Argentina
- ³ IFLP, Universidad Nacional de La Plata and CONICET, La Plata, Argentina
- ⁴ Instituto de Astronomía y Física del Espacio (IAFE, CONICET-UBA), Buenos Aires, Argentina
- ⁵ Instituto de Física de Rosario (IFIR) – CONICET/U.N.R. and Facultad de Ciencias Bioquímicas y Farmacéuticas U.N.R., Rosario, Argentina
- ⁶ Instituto de Tecnologías en Detección y Astropartículas (CNEA, CONICET, UNSAM), and Universidad Tecnológica Nacional – Facultad Regional Mendoza (CONICET/CNEA), Mendoza, Argentina
- ⁷ Instituto de Tecnologías en Detección y Astropartículas (CNEA, CONICET, UNSAM), Buenos Aires, Argentina
- ⁸ International Center of Advanced Studies and Instituto de Ciencias Físicas, ECyT-UNSAM and CONICET, Campus Miguelete – San Martín, Buenos Aires, Argentina
- ⁹ Laboratorio Atmósfera – Departamento de Investigaciones en Láseres y sus Aplicaciones – UNIDEF (CITEDEF-CONICET), Argentina
- ¹⁰ Observatorio Pierre Auger, Malargüe, Argentina
- ¹¹ Observatorio Pierre Auger and Comisión Nacional de Energía Atómica, Malargüe, Argentina
- ¹² Universidad Tecnológica Nacional – Facultad Regional Buenos Aires, Buenos Aires, Argentina
- ¹³ University of Adelaide, Adelaide, S.A., Australia
- ¹⁴ Université Libre de Bruxelles (ULB), Brussels, Belgium
- ¹⁵ Vrije Universiteit Brussels, Brussels, Belgium
- ¹⁶ Centro Federal de Educação Tecnológica Celso Suckow da Fonseca, Petropolis, Brazil
- ¹⁷ Instituto Federal de Educação, Ciência e Tecnologia do Rio de Janeiro (IFRJ), Brazil
- ¹⁸ Universidade de São Paulo, Escola de Engenharia de Lorena, Lorena, SP, Brazil
- ¹⁹ Universidade de São Paulo, Instituto de Física de São Carlos, São Carlos, SP, Brazil
- ²⁰ Universidade de São Paulo, Instituto de Física, São Paulo, SP, Brazil
- ²¹ Universidade Estadual de Campinas, IFGW, Campinas, SP, Brazil
- ²² Universidade Estadual de Feira de Santana, Feira de Santana, Brazil
- ²³ Universidade Federal de Campina Grande, Centro de Ciências e Tecnologia, Campina Grande, Brazil
- ²⁴ Universidade Federal do ABC, Santo André, SP, Brazil
- ²⁵ Universidade Federal do Paraná, Setor Palotina, Palotina, Brazil
- ²⁶ Universidade Federal do Rio de Janeiro, Instituto de Física, Rio de Janeiro, RJ, Brazil
- ²⁷ Universidade Federal do Rio de Janeiro (UFRJ), Observatório do Valongo, Rio de Janeiro, RJ, Brazil
- ²⁸ Universidade Federal Fluminense, EEIMVR, Volta Redonda, RJ, Brazil
- ²⁹ Universidad de Medellín, Medellín, Colombia
- ³⁰ Universidad Industrial de Santander, Bucaramanga, Colombia

- ³¹ Charles University, Faculty of Mathematics and Physics, Institute of Particle and Nuclear Physics, Prague, Czech Republic
- ³² Institute of Physics of the Czech Academy of Sciences, Prague, Czech Republic
- ³³ Palacky University, Olomouc, Czech Republic
- ³⁴ CNRS/IN2P3, IJCLab, Université Paris-Saclay, Orsay, France
- ³⁵ Laboratoire de Physique Nucléaire et de Hautes Energies (LPNHE), Sorbonne Université, Université de Paris, CNRS-IN2P3, Paris, France
- ³⁶ Univ. Grenoble Alpes, CNRS, Grenoble Institute of Engineering Univ. Grenoble Alpes, LPSC-IN2P3, 38000 Grenoble, France
- ³⁷ Université Paris-Saclay, CNRS/IN2P3, IJCLab, Orsay, France
- ³⁸ Bergische Universität Wuppertal, Department of Physics, Wuppertal, Germany
- ³⁹ Karlsruhe Institute of Technology (KIT), Institute for Experimental Particle Physics, Karlsruhe, Germany
- ⁴⁰ Karlsruhe Institute of Technology (KIT), Institut für Prozessdatenverarbeitung und Elektronik, Karlsruhe, Germany
- ⁴¹ Karlsruhe Institute of Technology (KIT), Institute for Astroparticle Physics, Karlsruhe, Germany
- ⁴² RWTH Aachen University, III. Physikalisches Institut A, Aachen, Germany
- ⁴³ Universität Hamburg, II. Institut für Theoretische Physik, Hamburg, Germany
- ⁴⁴ Universität Siegen, Department Physik – Experimentelle Teilchenphysik, Siegen, Germany
- ⁴⁵ Gran Sasso Science Institute, L'Aquila, Italy
- ⁴⁶ INFN Laboratori Nazionali del Gran Sasso, Assergi (L'Aquila), Italy
- ⁴⁷ INFN, Sezione di Catania, Catania, Italy
- ⁴⁸ INFN, Sezione di Lecce, Lecce, Italy
- ⁴⁹ INFN, Sezione di Milano, Milano, Italy
- ⁵⁰ INFN, Sezione di Napoli, Napoli, Italy
- ⁵¹ INFN, Sezione di Roma “Tor Vergata”, Roma, Italy
- ⁵² INFN, Sezione di Torino, Torino, Italy
- ⁵³ Istituto di Astrofisica Spaziale e Fisica Cosmica di Palermo (INAF), Palermo, Italy
- ⁵⁴ Osservatorio Astrofisico di Torino (INAF), Torino, Italy
- ⁵⁵ Politecnico di Milano, Dipartimento di Scienze e Tecnologie Aerospaziali, Milano, Italy
- ⁵⁶ Università del Salento, Dipartimento di Matematica e Fisica “E. De Giorgi”, Lecce, Italy
- ⁵⁷ Università dell’Aquila, Dipartimento di Scienze Fisiche e Chimiche, L’Aquila, Italy
- ⁵⁸ Università di Catania, Dipartimento di Fisica e Astronomia “Ettore Majorana”, Catania, Italy
- ⁵⁹ Università di Milano, Dipartimento di Fisica, Milano, Italy
- ⁶⁰ Università di Napoli “Federico II”, Dipartimento di Fisica “Ettore Pancini”, Napoli, Italy
- ⁶¹ Università di Palermo, Dipartimento di Fisica e Chimica “E. Segrè”, Palermo, Italy
- ⁶² Università di Roma “Tor Vergata”, Dipartimento di Fisica, Roma, Italy
- ⁶³ Università Torino, Dipartimento di Fisica, Torino, Italy
- ⁶⁴ Benemérita Universidad Autónoma de Puebla, Puebla, México
- ⁶⁵ Unidad Profesional Interdisciplinaria en Ingeniería y Tecnologías Avanzadas del Instituto Politécnico Nacional (UPIITA-IPN), México, D.F., México
- ⁶⁶ Universidad Autónoma de Chiapas, Tuxtla Gutiérrez, Chiapas, México
- ⁶⁷ Universidad Michoacana de San Nicolás de Hidalgo, Morelia, Michoacán, México
- ⁶⁸ Universidad Nacional Autónoma de México, México, D.F., México
- ⁶⁹ Universidad Nacional de San Agustín de Arequipa, Facultad de Ciencias Naturales y Formales, Arequipa, Peru
- ⁷⁰ Institute of Nuclear Physics PAN, Krakow, Poland
- ⁷¹ University of Łódź, Faculty of High-Energy Astrophysics, Łódź, Poland
- ⁷² Laboratório de Instrumentação e Física Experimental de Partículas – LIP and Instituto Superior Técnico – IST, Universidade de Lisboa – UL, Lisboa, Portugal
- ⁷³ “Horia Hulubei” National Institute for Physics and Nuclear Engineering, Bucharest-Magurele, Romania
- ⁷⁴ Institute of Space Science, Bucharest-Magurele, Romania
- ⁷⁵ University Politehnica of Bucharest, Bucharest, Romania
- ⁷⁶ Center for Astrophysics and Cosmology (CAC), University of Nova Gorica, Nova Gorica, Slovenia
- ⁷⁷ Experimental Particle Physics Department, J. Stefan Institute, Ljubljana, Slovenia

- ⁷⁸ Universidad de Granada and C.A.F.P.E., Granada, Spain
⁷⁹ Instituto Galego de Física de Altas Enerxías (IGFAE), Universidade de Santiago de Compostela, Santiago de Compostela, Spain
⁸⁰ IMAPP, Radboud University Nijmegen, Nijmegen, The Netherlands
⁸¹ Nationaal Instituut voor Kernfysica en Hoge Energie Fysica (NIKHEF), Science Park, Amsterdam, The Netherlands
⁸² Stichting Astronomisch Onderzoek in Nederland (ASTRON), Dwingeloo, The Netherlands
⁸³ Universiteit van Amsterdam, Faculty of Science, Amsterdam, The Netherlands
⁸⁴ Case Western Reserve University, Cleveland, OH, USA
⁸⁵ Colorado School of Mines, Golden, CO, USA
⁸⁶ Department of Physics and Astronomy, Lehman College, City University of New York, Bronx, NY, USA
⁸⁷ Michigan Technological University, Houghton, MI, USA
⁸⁸ New York University, New York, NY, USA
⁸⁹ University of Chicago, Enrico Fermi Institute, Chicago, IL, USA
⁹⁰ University of Delaware, Department of Physics and Astronomy, Bartol Research Institute, Newark, DE, USA
⁹¹ University of Wisconsin-Madison, Department of Physics and WIPAC, Madison, WI, USA

- ^a Louisiana State University, Baton Rouge, LA, USA
^b also at University of Bucharest, Physics Department, Bucharest, Romania
^c School of Physics and Astronomy, University of Leeds, Leeds, United Kingdom
^d now at Agenzia Spaziale Italiana (ASI). Via del Politecnico 00133, Roma, Italy
^e Fermi National Accelerator Laboratory, Fermilab, Batavia, IL, USA
^f now at Graduate School of Science, Osaka Metropolitan University, Osaka, Japan
^g now at ECAP, Erlangen, Germany
^h Max-Planck-Institut für Radioastronomie, Bonn, Germany
ⁱ also at Kapteyn Institute, University of Groningen, Groningen, The Netherlands
^j Colorado State University, Fort Collins, CO, USA
^k Pennsylvania State University, University Park, PA, USA

Acknowledgments

The successful installation, commissioning, and operation of the Pierre Auger Observatory would not have been possible without the strong commitment and effort from the technical and administrative staff in Malargüe. We are very grateful to the following agencies and organizations for financial support:

Argentina – Comisión Nacional de Energía Atómica; Agencia Nacional de Promoción Científica y Tecnológica (ANPCyT); Consejo Nacional de Investigaciones Científicas y Técnicas (CONICET); Gobierno de la Provincia de Mendoza; Municipalidad de Malargüe; NDM Holdings and Valle Las Leñas; in gratitude for their continuing cooperation over land access; Australia – the Australian Research Council; Belgium – Fonds de la Recherche Scientifique (FNRS); Research Foundation Flanders (FWO); Brazil – Conselho Nacional de Desenvolvimento Científico e Tecnológico (CNPq); Financiadora de Estudos e Projetos (FINEP); Fundação de Amparo à Pesquisa do Estado de Rio de Janeiro (FAPERJ); São Paulo Research Foundation (FAPESP) Grants No. 2019/10151-2, No. 2010/07359-6 and No. 1999/05404-3; Ministério da Ciência, Tecnologia, Inovações e Comunicações (MCTIC); Czech Republic – Grant No. MSMT CR LTT18004, LM2015038, LM2018102, CZ.02.1.01/0.0/0.0/16_013/0001402, CZ.02.1.01/0.0/0.0/18_046/0016010 and CZ.02.1.01/0.0/0.0/17_049/0008422; France – Centre de Calcul IN2P3/CNRS; Centre National de la Recherche Scientifique (CNRS); Conseil Régional Ile-de-France; Département Physique Nucléaire et Corpusculaire (PNC-IN2P3/CNRS); Département Sciences de l’Univers (SDU-INSU/CNRS); Institut Lagrange de Paris (ILP) Grant No. LABEX ANR-10-LABX-63 within the Investissements d’Avenir Programme Grant No. ANR-11-IDEX-0004-02; Germany – Bundesministerium für Bildung und Forschung (BMBF); Deutsche Forschungsgemeinschaft (DFG); Finanzministerium Baden-Württemberg; Helmholtz Alliance for Astroparticle Physics (HAP); Helmholtz-Gemeinschaft Deutscher Forschungszentren (HGF); Ministerium für Kultur und Wissenschaft des Landes Nordrhein-Westfalen; Ministerium für Wissenschaft, Forschung und Kunst des Landes Baden-Württemberg; Italy – Istituto Nazionale di Fisica Nucleare (INFN); Istituto Nazionale di Astrofisica (INAF); Ministero dell’Università e della Ricerca (MUR); CETEMPS Center of Excellence; Ministero degli Affari Esteri (MAE), ICSC Centro Nazionale di Ricerca in High Performance Computing, Big Data

and Quantum Computing, funded by European Union NextGenerationEU, reference code CN_00000013; México – Consejo Nacional de Ciencia y Tecnología (CONACYT) No. 167733; Universidad Nacional Autónoma de México (UNAM); PAPIIT DGAPA-UNAM; The Netherlands – Ministry of Education, Culture and Science; Netherlands Organisation for Scientific Research (NWO); Dutch national e-infrastructure with the support of SURF Cooperative; Poland – Ministry of Education and Science, grants No. DIR/WK/2018/11 and 2022/WK/12; National Science Centre, grants No. 2016/22/M/ST9/00198, 2016/23/B/ST9/01635, 2020/39/B/ST9/01398, and 2022/45/B/ST9/02163; Portugal – Portuguese national funds and FEDER funds within Programa Operacional Factores de Competitividade through Fundação para a Ciência e a Tecnologia (COMPETE); Romania – Ministry of Research, Innovation and Digitization, CNCS-UEFISCDI, contract no. 30N/2023 under Romanian National Core Program LAPLAS VII, grant no. PN 23 21 01 02 and project number PN-III-P1-1.1-TE-2021-0924/TE57/2022, within PNCDI III; Slovenia – Slovenian Research Agency, grants P1-0031, P1-0385, I0-0033, N1-0111; Spain – Ministerio de Economía, Industria y Competitividad (FPA2017-85114-P and PID2019-104676GB-C32), Xunta de Galicia (ED431C 2017/07), Junta de Andalucía (SOMM17/6104/UGR, P18-FR-4314) Feder Funds, RENATA Red Nacional Temática de Astropartículas (FPA2015-68783-REDT) and María de Maeztu Unit of Excellence (MDM-2016-0692); USA – Department of Energy, Contracts No. DE-AC02-07CH11359, No. DE-FR02-04ER41300, No. DE-FG02-99ER41107 and No. DE-SC0011689; National Science Foundation, Grant No. 0450696; The Grainger Foundation; Marie Curie-IRSES/EPLANET; European Particle Physics Latin American Network; and UNESCO.